



CYGNET DEVELOPMENT SERVICES LTD

Computational Fluid Dynamics Modelling

Filename: Okazaki Report_V3_TO_ApRE_1_300608
Version: 3
Author: T. Oakes
Date: 30/06/2008

The status and control of this document is given by the file name.

File name convention - Document name_Version number_Author_Draft/Approved_Security level_date

Author – Initials of the originator of the file.

Draft / Approved status – Draft (D) or Approved (Ap and the initials of the approver).

Security level - 0 – Public, 1 – NDA, 2 – Suppliers, 3 – Collaborators, 4 – Some Swanturbines staff, 5 - Directors

Date – six digit date code.

Description and document purpose:

Associated Files:

Predecessor Files:

Quality Assurance			
Date	Revision	Author	Approved

Cygnnet Development Services Ltd
Swanturbines
Digital Technium
Singleton Park
Swansea
SA2 8PP

Telephone: 01792 295217
Fax: 01792 295676
Email: enquires@cygnetds.co.uk
Company Reg No.: 6586742
VAT No. 933530928

1 Executive Summary

Okazaki have developed a new design of thermowell with helical strakes that are intended to completely remove vortex induced resonance failures of thermowells in service.

This report outlines the findings of a comparative CFD analysis that was completed on behalf of Okazaki. The report presents the results in a clear and understandable way such that they can be used by Okazaki to explain the differences in design to potential customers.

2 Contents

1	Executive Summary.....	2
2	Contents	2
3	Introduction.....	3
4	Methodology.....	3
4.1	CFD Parameters	3
4.1.1	Model Geometry	3
4.1.2	Mesh	3
4.1.3	Convergence Criteria.....	5
4.1.4	Environmental Conditions.....	5
4.1.5	Computational Control	5
5	Results.....	6
5.1	Smooth Thermowell	7
5.1.1	Velocity Plots (Top View).....	7
5.1.2	Flow Stream Lines (Top View).....	8
5.1.3	Comparative Surface Pressure Distribution (Top View).....	9
5.1.4	Surface Pressure Distribution (Front View)	9
5.1.5	Vertical Velocity Distribution (Front View).....	9
5.2	Straked Thermowell	10
5.2.1	Velocity Plots (Top View).....	10
5.2.2	Flow Stream Lines (Top View).....	11
5.2.3	Surface Pressure Distribution (Top View).....	12
5.2.4	Vertical Velocity Distribution (Front View).....	12
6	Discussion	12
6.1	Flow Behaviour.....	12
6.1.1	Smooth Thermowell Plots	12
6.1.2	Straked Thermowell Plots	13
6.1.3	Thermowell Comparisons	13
6.2	Frequency Analysis	14
6.2.1	Smooth Thermowell.....	14
6.2.2	Straked Thermowell	15
6.2.3	Frequency Comparison.....	15
6.2.4	Model Frequency	15
7	Conclusions	16
7.1.1	Summarised Conclusions	16
8	References	17
9	Liability/Indemnity	17
10	Appendix.....	18
10.1	Appendix – Drawing Number T4B17821.....	18
10.2	Appendix – Drawing Number T4B17822.....	19
10.3	Appendix – Strouhal Frequency.....	20
10.4	Appendix – Smooth Thermowell Velocity Plots	21
10.5	Appendix – Straked Thermowell Velocity Plots	22

3 Introduction

This report is intended to present the findings of the comparative CFD analysis completed on behalf of Okazaki. Two distinct time dependent studies have been completed; one for a standard, smooth cylindrical thermowell and one for a thermowell equipped with helical strakes matching Okazaki's design. The report outlines the procedure adopted, the results with summarising discussion and conclusions.

4 Methodology

It was decided that DS SolidWorks would be utilised as an analysis tool for the problem exploiting the FloWorks module to complete the CFD study. The module is capable of solving flow problems using a SolidWorks model based upon a range of parameters. The SolidWorks models of each thermowell were taken from the drawings provided, T4B17821 and T4B17822 as shown in appendix 10.1 and 10.2 respectively.

The FloWorks module required a number of parameters to describe the fluid environment and the modelling procedure. These factors were established from experience of fluid dynamics and the software. A series of coarse, two dimensional studies were completed to ascertain further information regarding the anticipated flow behaviour and to assist in some crucial parameter settings. The following sections outline the modelling parameters.

With both models constructed with suitable computational domains and meshes the two problems were solved independently using an iterative, time stepped scheme solving the full laminar and turbulent Navier Stokes equations.

The results of each study are presented in a range of forms within the results section.

4.1 CFD Parameters

4.1.1 Model Geometry

The exact geometries of the models were taken from design drawings provided by Okazaki. These were developed within SolidWorks as three dimensional, solid models. Two examples of strake features are presented within T4B17822 and it was decided with Okazaki to model the machined strakes as opposed to the less defined weld wire strakes. Figure 1 shows the classical thermowell and the straked thermowell solid models.



Figure 1 – Thermowell CAD Models

4.1.2 Mesh

A computational mesh was constructed for each of the thermowell geometries, each based on similar criteria. The boundaries of the mesh were designated by the pre-described computational domain which was set based upon 2D investigations into the range and extent of significant flow phenomena. This region was designed to be as small as possible without infringing upon flow behaviour of interest to the study. The 2D studies also demonstrated that both models required a high mesh resolution in the wake stream as well as at the solid/fluid interface due to the activity highlighted.

One key issue concerning the computational domain was the depth of thermowell it was possible to model accurately. It was found in the initial scope, that tip features would be very memory intensive and retract from the vortex phenomena that were the primary goal of the study. A series of short studies optimised the required depth of the domain in order to accurately capture the 3D effects of strakes. Figures 2 and 3 show the size of the computational domain for both the classical and straked thermowells.

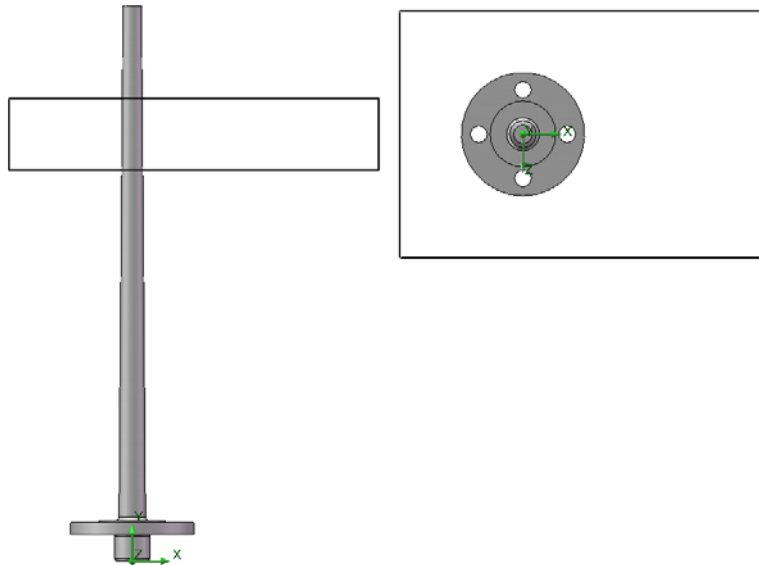


Figure 2 – Classic thermowell computational domain

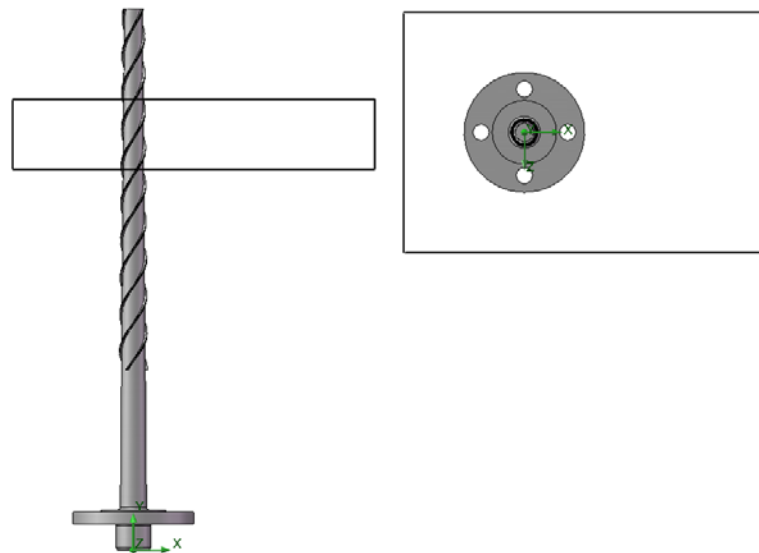


Figure 3 – Straked thermowell computational domain

In order to capture small surface features and improve the overall accuracy of the modelling, automatic surface refinement was applied to the mesh. This process highlighted the fluid/solid surface and refined the mesh resolution locally during the calculation process. This process was computationally costly but was deemed worthwhile for enhanced calculation around strake features. Both models were given the same

initial mesh structure but the automated refinement resulted in meshes individualised for each of the thermowell geometries. Figure 4 shows the pre-described mesh structure prior to surface refinement.

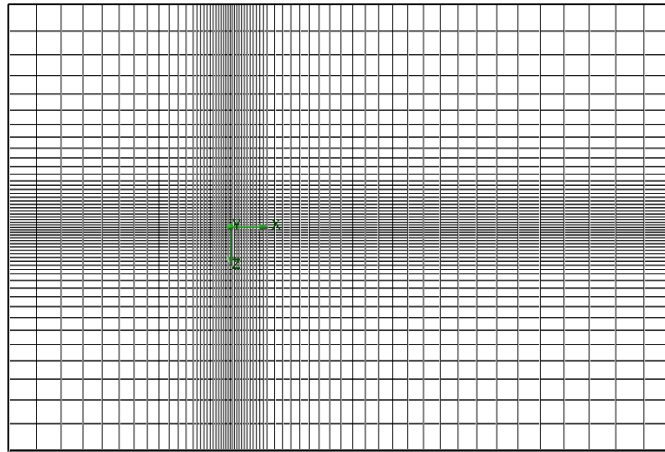


Figure 4 – Initial Mesh Construction

4.1.3 Convergence Criteria

The convergence criteria provided an important parameter for the iterative solution. Vortex behaviour is primarily identified by the swirl of fluid and the relative velocity changes. For this reason, it was decided to include the conditions shown below to ensure that the best results were achieved:

- Average Velocity
- Average Static Pressure
- Max Total Pressure
- Max Velocity
- Max X Velocity
- Max Y Velocity
- Max Z Velocity

These seven criteria were considered more than sufficient to provide high quality results for the type of problem investigated.

4.1.4 Environmental Conditions

The following outlines the environmental parameters of the study.

Flow speed:	8.15m/s
Pressure:	10 MPa
Fluid:	Water
Wall thermal condition:	Default Adiabatic wall
Temperature:	293.2 K
Turbulence intensity:	0.1%
Turbulence length:	0.001m

4.1.5 Computational Control

In order to establish the discretization of results required to capture vortex behaviour it was necessary to compute the approximate shedding frequency. This was done using Reynolds and Strouhal number approximations:

$$Re = \frac{DU}{\nu}$$

Where:

$$D = 0.022 \text{ m}$$

$$U = 8.15 \text{ m/s}$$

$$\nu = 1.05 \times 10^{-6} \text{ m}^2/\text{s}$$

$$Re = \frac{0.022 \times 8.15}{1.05 \times 10^{-6}} = 170762$$

From experimental results it can be assumed that this Reynolds number equates to a Strouhal number of 0.2 [Appendix 10.3].

$$St = \frac{f_v \times D}{U}$$

$$f_v = \frac{St \times U}{D}$$

$$f_v = \frac{0.2 \times 8.15}{0.022} = 74.1 \text{ Hz}$$

Due to the high frequency of vortex shedding that was predicted, the analysis was run for a total physical time of 0.3 seconds. This was predicted to demonstrate approximately 20 vortex cycles, more than enough to illustrate the behaviour. Therefore, 0.3 seconds of physical time was the specified finishing criteria for each model run. Data was captured every 0.001 second giving a total of 300 time slices. This would mean that there were approximately 10 data sets per vortex cycle which was deemed to be sufficient to capture vortex phenomena.

5 Results

Due to the time dependent nature of the flow behaviour, results are presented as plots over at least 3 time steps to illustrate any dynamic variations. To examine 3D effects some plots have been replicated over numerous planes. It was found that 4 planes were sufficient to capture the behaviour of a straked thermowell and 2 for a smooth thermowell. Figure 5 illustrates the cut planes in both models. The global coordinate system is also shown and the flow is prescribed to act in the positive x direction.

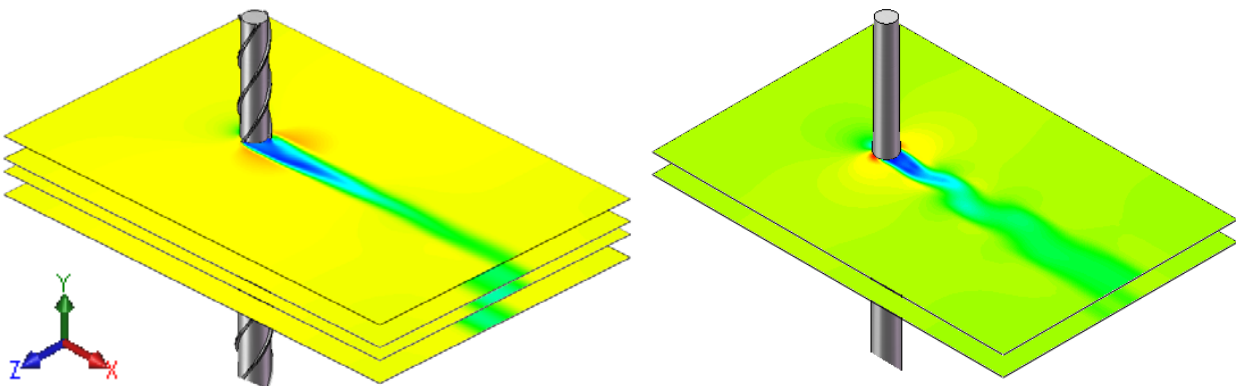


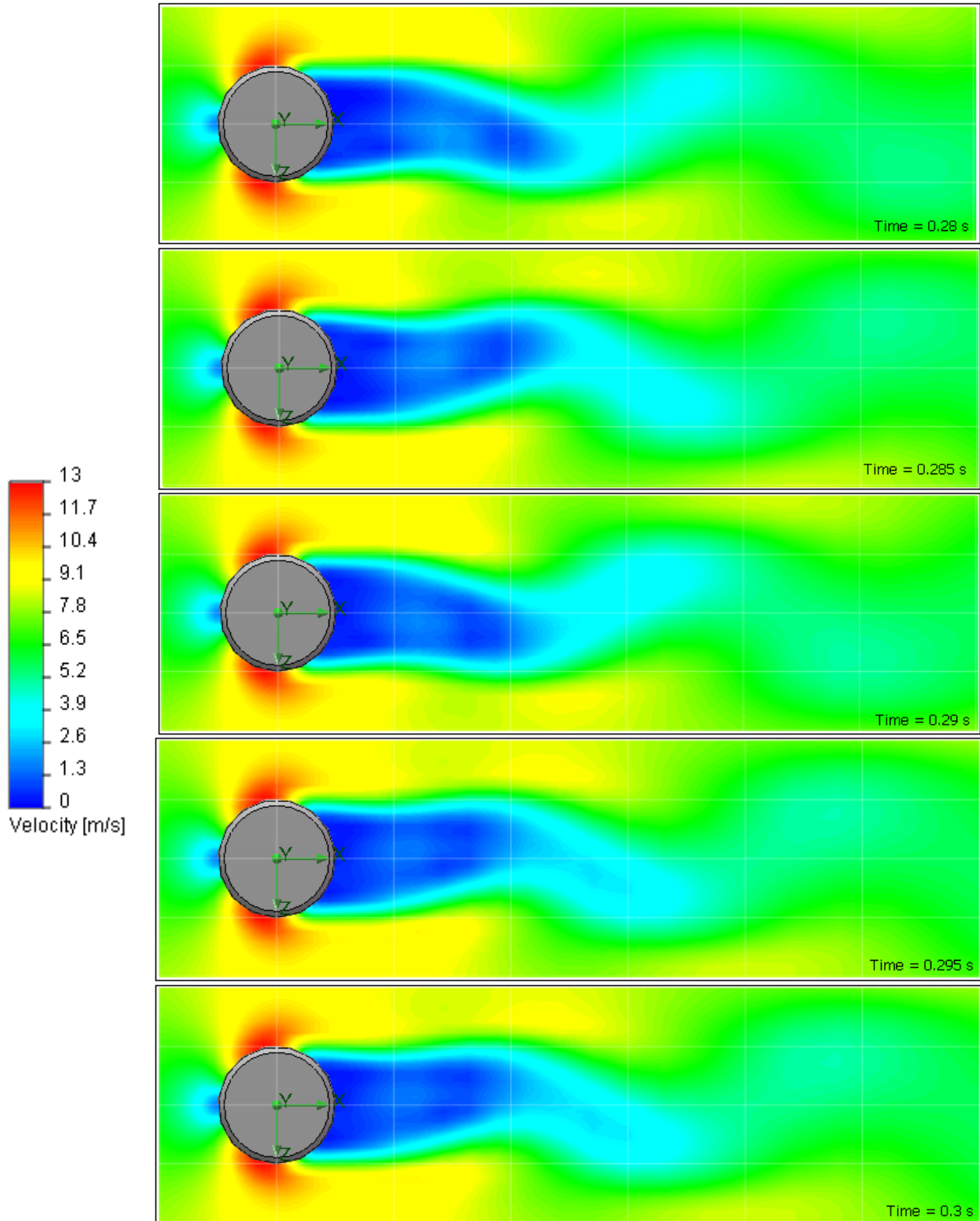
Figure 5 – Model cut planes utilised to visualise 3D flow variations

Each model has 300 data sets equally spaced across the 0.3 seconds of physical time. At each time step there are a large number of plots available to present the findings. This leads to a significantly large range of possible result plots. For this reason the report only presents the most pertinent results to examine the behaviour but in no way attempts to show the full findings. Extensive investigation and result visualisation has been completed to ensure that what is shown accurately presents the predicted phenomena of interest.

5.1 Smooth Thermowell

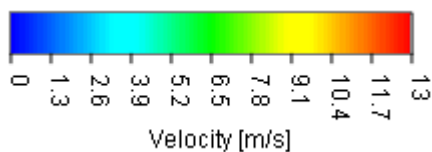
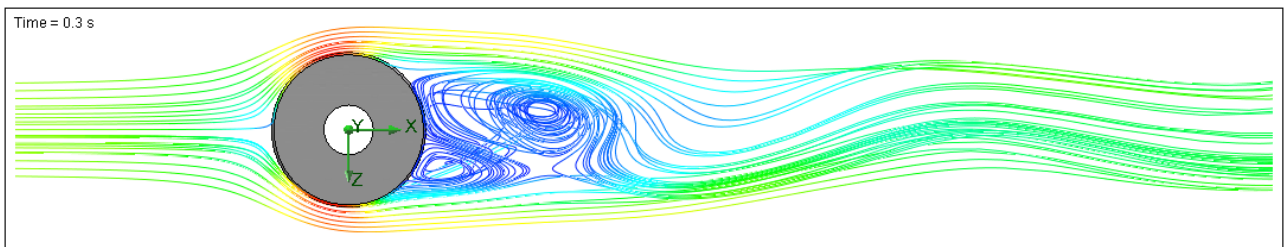
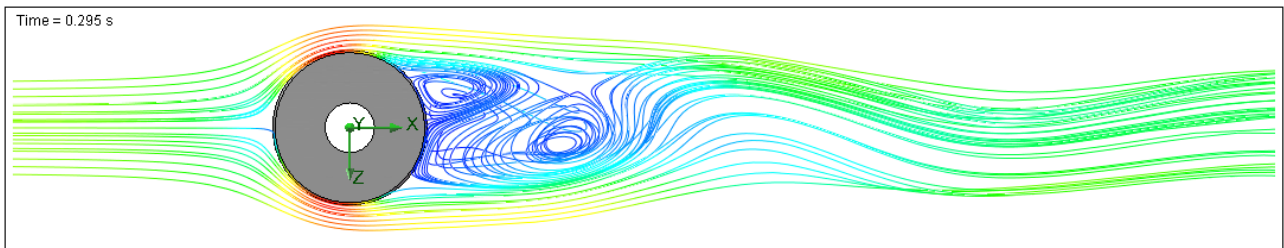
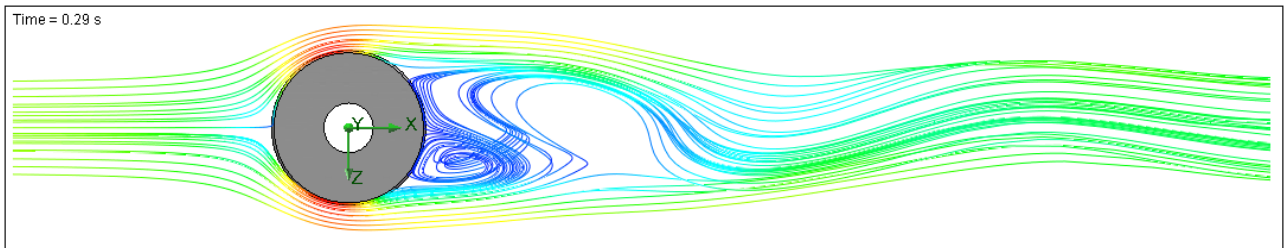
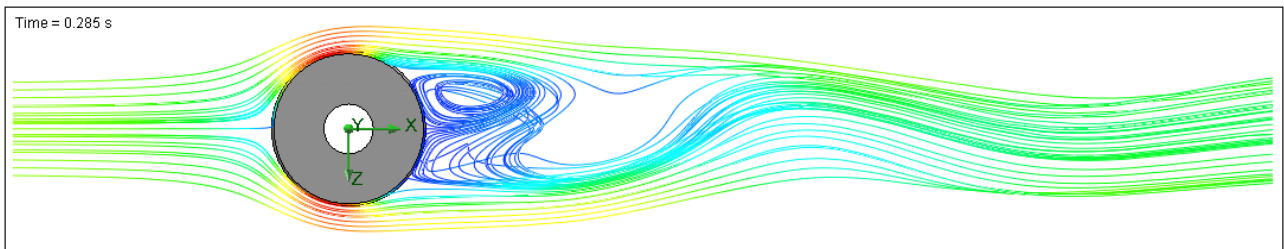
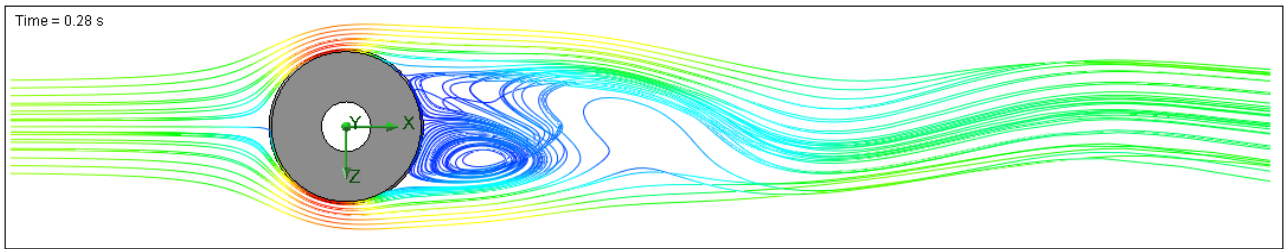
The results for the smooth, standard design of thermowell are presented in this section. In order to ascertain if the behaviour varied through the flow planes (in the y direction) results were observed over a range of time steps at various depths. It was found that the flow behaviour calculated was consistent through the depth of the thermowell. For this reason, the results shown here are for a single flow plane.

5.1.1 Velocity Plots (Top View)

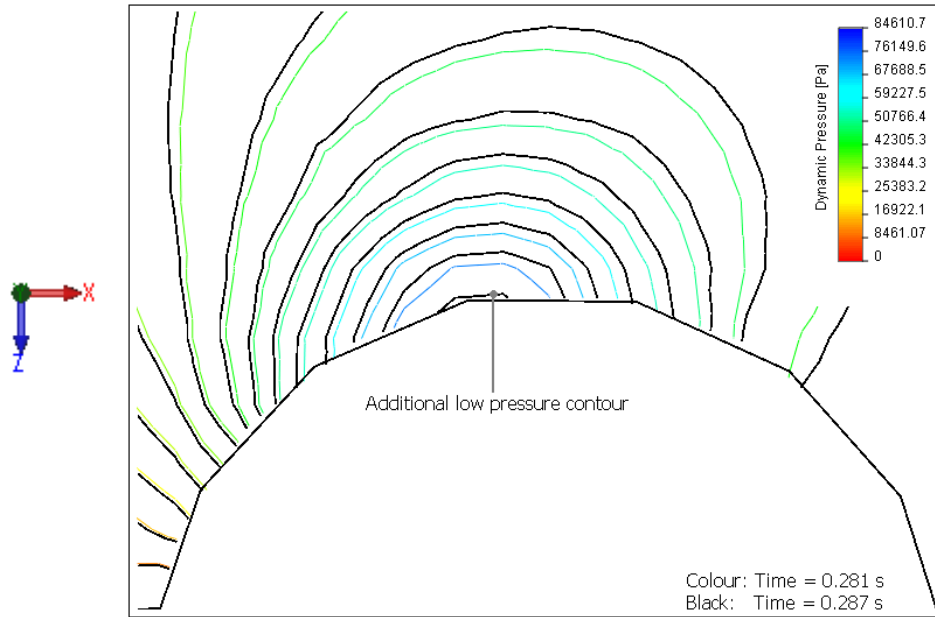


Appendix 10.4 shows the velocity profile over a larger domain and at two differing depths of cut. This gives a broader illustration of the overall flow behaviour and also shows how the shedding behaviour is replicated across the depth of the thermowell.

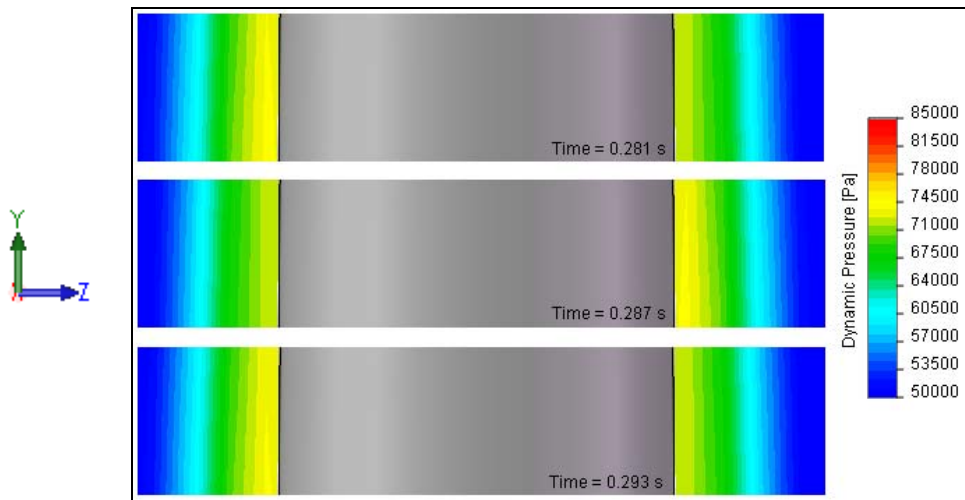
5.1.2 Flow Stream Lines (Top View)



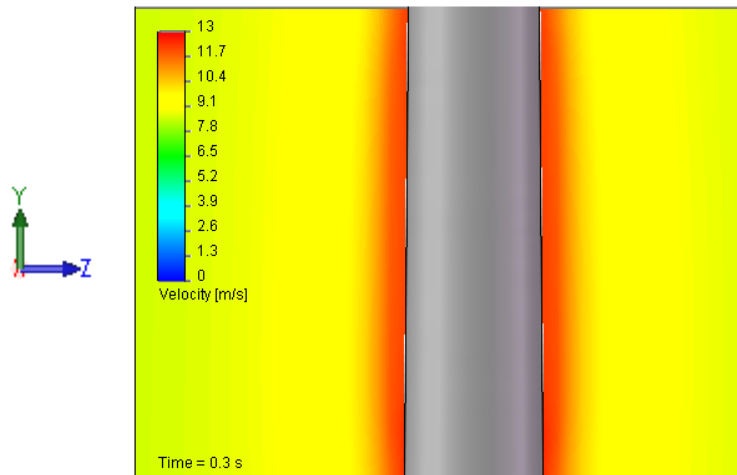
5.1.3 Comparative Surface Pressure Distribution (Top View)



5.1.4 Surface Pressure Distribution (Front View)



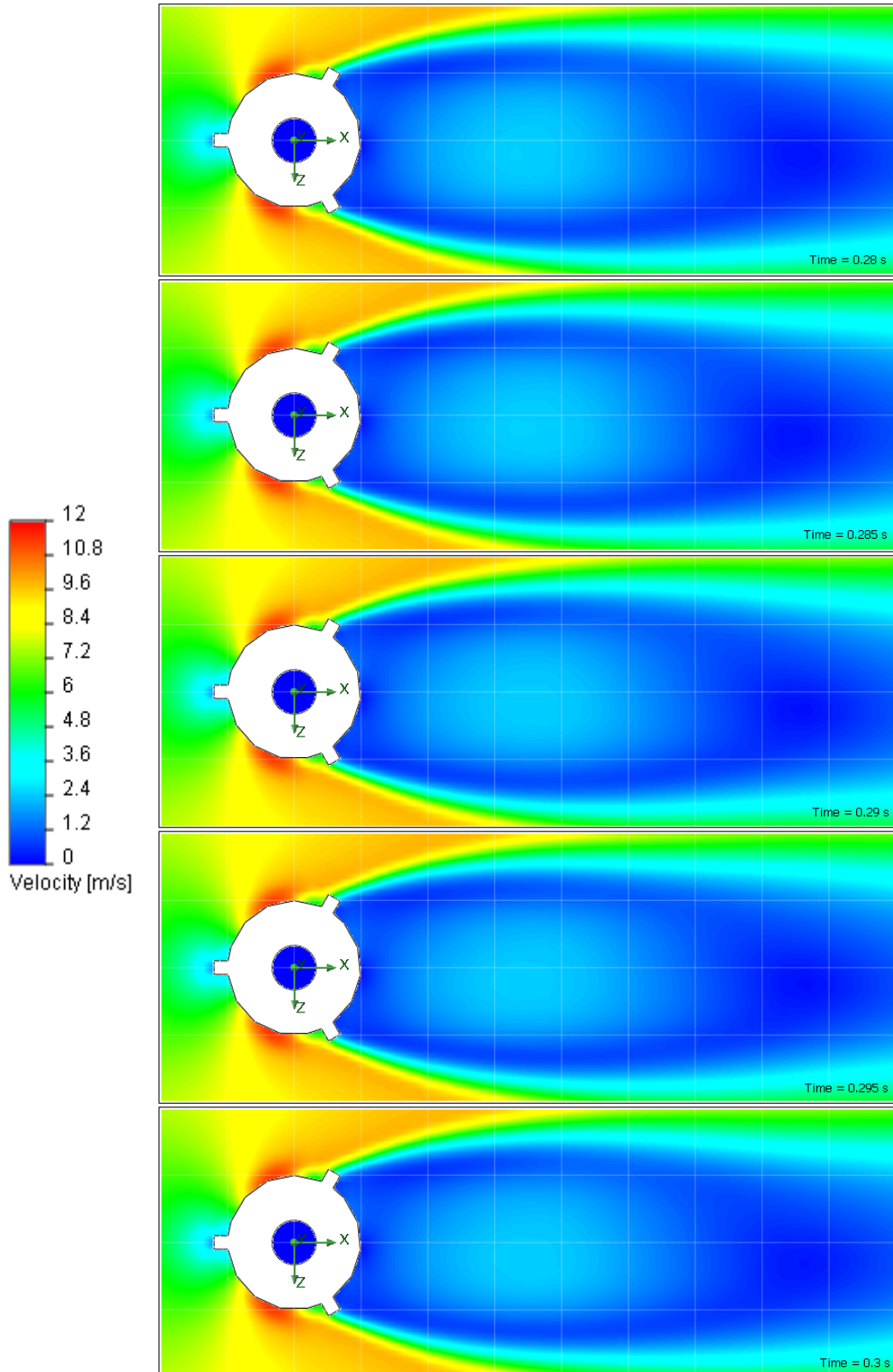
5.1.5 Vertical Velocity Distribution (Front View)



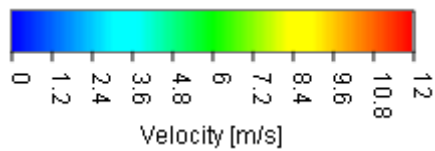
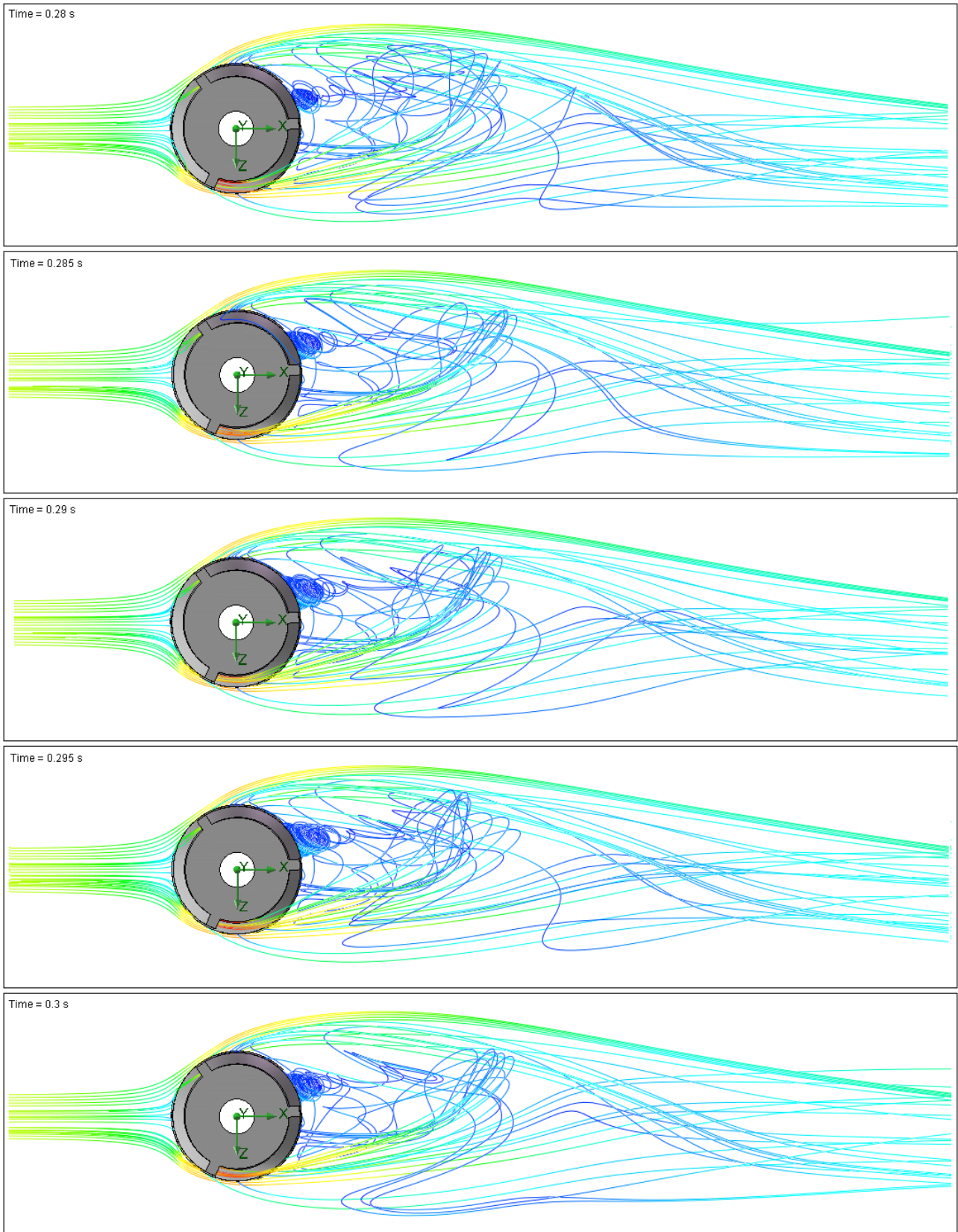
5.2 Straked Thermowell

Similar to the smooth thermowell, results for the straked device are presented for one plane. The behaviour of flow varied significantly across planes yet it was observed that in each plane the dynamic behaviour was stable and showed little or no variation with time. Appendix 10.5 shows velocity plots over 4 planes.

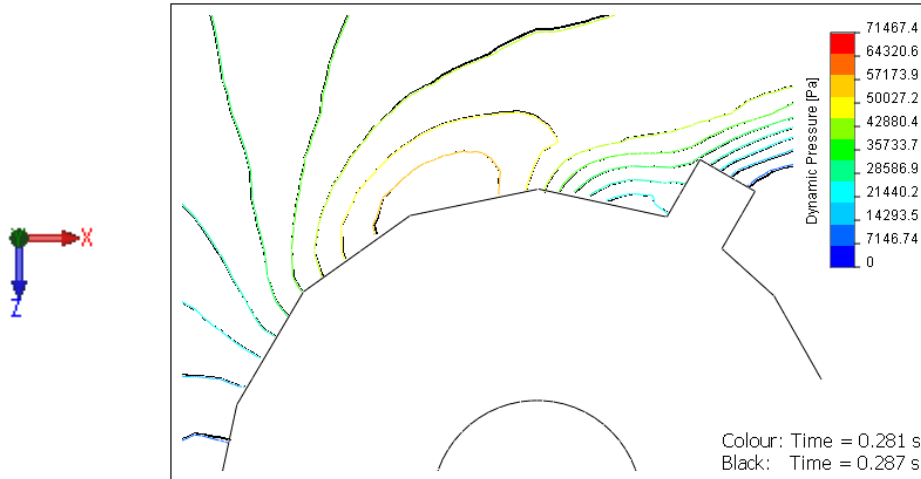
5.2.1 Velocity Plots (Top View)



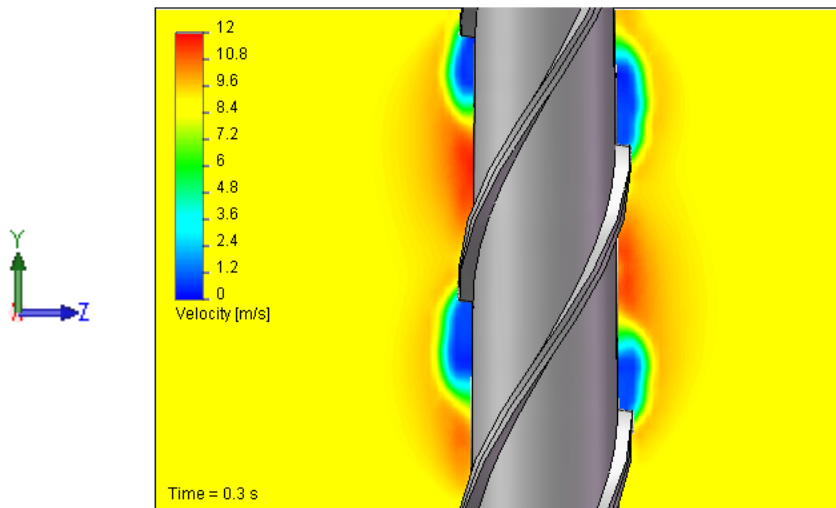
5.2.2 Flow Stream Lines (Top View)



5.2.3 Surface Pressure Distribution (Top View)



5.2.4 Vertical Velocity Distribution (Front View)



6 Discussion

6.1 Flow Behaviour

Broadly speaking the CFD results have provided an excellent opportunity to observe the flow characteristics of both thermowell designs. Visual comparison of the plots demonstrates a stark difference in the way in which the two designs affect the flow.

6.1.1 Smooth Thermowell Plots

The velocity plots displayed in 5.1.1 clearly demonstrate that a von Kármán street shedding phenomena occurs in the wake region of the standard thermowell. Examination of the data over a range of time steps identified that this shedding was consistent and regular. The results downstream help visualise the oscillating phenomenon that is presented from this behaviour by showing the cyclic variation of vortex shedding from one side to the other. The flow streamlines plotted as 5.1.2 help to identify the vortex behaviour further and show the considerable whirl created in the vortex regions.

Theoretically, it would be expected that the shallow taper would give differing shedding frequencies along the length of the thermowell. With this in mind, the data was observed over numerous planes and it was found that the vortex shedding occurred simultaneously along the full length of the assessed section. This basically found that the shedding frequency was consistent along the length of the well regardless of the tapered

geometry. Additional plots showing this are presented in appendix 10.4. It is proposed that flow shear effects along the length of the well (in the y direction) provide the mechanism that links the shedding and maintains it's consistency.

The velocity plot 5.1.5 shows the flow velocity profile along the full length of the studied section. This also helps to demonstrate that flow behaviour is replicated in all planes through the well length. From these observations, it can be assumed that any cyclic variations in pressure (the drive behind vortex induced vibrations) can be extrapolated along the full length of the thermowell within a given flow field.

5.1.3 presents overlaid pressure contours at two time steps in one plane. The plot is presented in this way to show the time dependent pressure changes that are occurring in the pressure field around the thermowell. The coloured lines show the pressure isolines at 0.281 seconds and the black lines show them at 0.287 seconds. The two data sets are chosen at these time steps as they are approximately half a frequency cycle apart. It is noted on the plot that as the time progresses an additional low pressure contour is identified. This shows that the thermowell experiences a marked drop in pressure through the time step. 5.1.4 shows the pressure variation as viewed from the front and illustrates this behaviour. These results show that coinciding with a pressure drop on one side of the well there is a relative pressure rise on the other. This gives rise to a net pressure gradient in the z direction. The CFD results have provided excellent visualisation of the mechanism behind vortex induced vibrations as has already been widely studied and reported.

The aim of the study was to visualise the flow behaviour in order to provide comparison in designs. It's considered that the behaviour observed here presents a fatigue concern. Further work would have to be completed to ascertain the magnitude of the loadings yet it is noted that a relatively high frequency, cyclic loading has been approximated by the study.

6.1.2 Straked Thermowell Plots

The velocity plots for the straked thermowell are displayed in 5.2.1. The wake region shows no regular behaviour patterns and no indication of vortex shedding. Due to the design of the strakes it was apparent that significant cross plane flow effects would occur and so the velocity plots were observed over numerous planes. Appendix 10.5 shows velocity plots over 4 depths and 3 time steps. It was found that there were significant variations in the flow behaviour along the length of the well, yet in all planes the flow was considered to be stable and presented no signs of regular vortex shedding. The dynamic pressure behaviour was consistent and showed little or no variations.

The streamline plots, presented as 5.2.2, show that the flow in the wake region is relatively disturbed presenting a lot of turbulent activity. Observing the streamlines showed that the strakes promoted significant cross planes flows whilst also diverting boundary layer flows from their normal course. It's thought that this mechanism promotes significant disturbance as to hinder vortex formation mechanisms.

Similar to the standard thermowell design, 5.2.3 shows overlaid pressure contours over two time steps. This was completed for a range of time steps and in all cases the pressure field showed no noticeable change. This shows that the driving mechanism for vortex induced vibrations appears not to be present for the thermowell equipped with helical strakes.

5.2.4 presents the velocity profile around the well as viewed from the front. This plot conveniently demonstrates the flow variations along the length of the thermowell. A point of note is that the behaviour replicates itself along the well which implies that the results for the reduced section can be extrapolated over the full length of thermowell within the flow field. The helical strakes appear to 'twist' the flow causing a shift in the velocities and also the pressure field. This non-uniform distribution may also be another mechanism by which helical strakes act to reduce and remove vortex induced vibrations. Velocities are proportional to dynamic pressures and therefore the offset and varying velocity field along the well length can equally be interpreted as pressure. For any vortex street to excite a structure, net pressure changes must occur over the full structure. The pressure variations present no net pressure gradient and the overall effect is for the 'twisted' flow behaviour to cancel out on both sides of the well. This does show that strakes must cover a significant length in order not to create a constant, out of balance pressure gradient.

6.1.3 Thermowell Comparisons

The main purpose of the study was to compare the changes in flow behaviours as a result of adding helical strakes to a thermowell. In the previous section, the 3D effects of the flow in the y direction have been

discussed. While changes occur for the straked well the overall flow behaviours can be compared looking in a single flow plane. Figure 6 shows the streamlines in the wake region of both the standard and the straked thermowells.

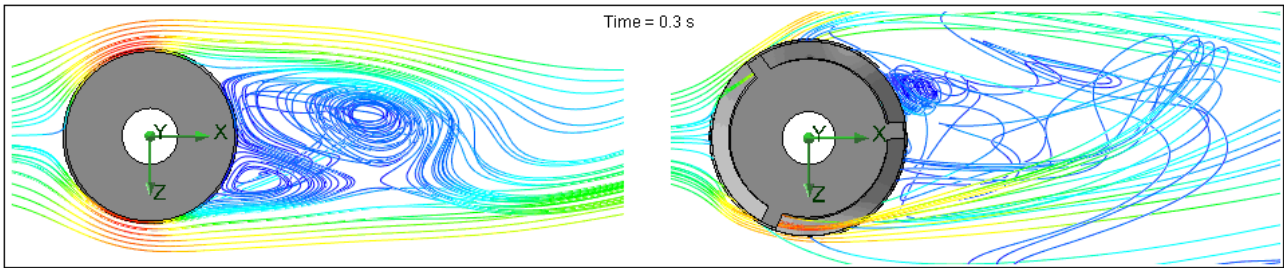


Figure 6 – Comparative streamline plot

Comparing the plots side by side clearly shows the dramatic effect that the strakes have. As has already been discussed the standard well presents classic shedding behaviour whereas the straked device presents no regular flow behaviour. It appears to be the strakes abilities to disturb the flow that interrupts regular vortex formation. While a small vortex site is observed in the wake of the straked well, this appears to be a localised stagnation point and doesn't seem to shed.

The most significant and obvious comparison that can be made is that regarding the pressure fields. For the standard well design, an oscillating pressure field is found around the structure. The straked device displays a constant and stable pressure field presenting no dynamic variations. As this pressure is the source of vortex induced vibrations it can be assumed that the straked device would experience a significant improvement compared to the standard thermowell.

6.2 Frequency Analysis

The predominant drive behind this study was to investigate the vortex behaviour of two thermowells because of the problems associated with vortex induced vibrations. In order to comprehensively cover the problem it's important to fully understand the dynamic behaviour of the thermowells in question. The Power Test Code [1] considers vortex behaviour with some coarse approximations to a designs resonance and utilises a frequency ratio as a limitation to applications. For this reason both designs of well have been computationally assessed to calculate their respective natural frequencies. A finite element method was adopted within SolidWorks to compute the natural frequencies and the mode shapes of the thermowells.

6.2.1 Smooth Thermowell



6.2.2 Straked Thermowell



6.2.3 Frequency Comparison

The power code calculation gives the lowest natural frequency of the standard thermowell as 68.5Hz. The FEA completed gives the figure as 90.3Hz. This presents a significant difference and highlights that the power code design rules involve assumptions which can and do lead to significant inaccuracies.

6.2.4 Model Frequency

The study demonstrated that no clear vortex shedding or any regular cyclic behaviour was observed for the thermowell equipped with helical strakes for this reason the CFD predicted shedding frequency was only obtained for a cylindrical thermowell without helical strakes.

In order to ascertain the frequency of shedding predicted by the model, streamlines were plotted around the thermowell. As only a portion of an operating thermowell is placed within the flow was decided to observe the shedding in the plane near the tip where the thermowell measured 20mm in diameter. The theoretical shedding frequency is calculated below

$$Re = \frac{0.02 \times 8.15}{1.05 \times 10^{-6}} = 155238$$

From experimental results it can be assumed that this Reynolds number equates to a Strouhal number of 0.2 [Appendix 10.3].

$$f_v = \frac{0.2 \times 8.15}{0.02} = 81.5Hz$$

From the model results, vortex cycles were counted over the last 0.1 seconds of the study. This time span demonstrated approximately 9 shedding cycles which equates to a frequency of 90Hz. It is important to note that errors in the source and graphical interpretation of the Strouhal number could have a significant effect on the predicted shedding frequency. The Power Test Code [1] states that 'the value of the Strouhal number is generally taken as 0.22'. If this were the case then the vortex shedding frequency would be predicted as

$$f_v = \frac{0.22 \times 8.15}{0.02} = 89.65 \text{ Hz}$$

In this case excellent agreement is observed. It should also be considered that the taper of the thermowell may give rise to 3D effects resulting in cross plane velocity flows. This taper effect would invalidate the theory of shedding frequency which effectively assumes a cylinder of uniform cross section.

It's not recommended that this type of CFD modelling is used to predict shedding frequencies without extensive validation but the model does appear to show good agreement with the theory and would consider 3D taper effects where the basic theory makes no account.

7 Conclusions

The CFD results have clearly presented and helped to visualise the flow behaviour of both a standard design, smooth thermowell and a thermowell equipped with helical strakes.

The standard thermowell demonstrated the documented phenomenon of oscillating vortex shedding also known as a von Kármán street. This behaviour was observed best in a flow velocity plot and as flow streamlines. It was found that the shedding behaviour occurred simultaneously along the length of the thermowell (the shedding frequency didn't vary in the y direction) which it is predicted would give rise to significant pressure variations thus providing the drive to cause vibrations. The CFD predicted a shedding frequency of approximately 90Hz which showed good agreement with theory based upon Strouhal number.

It was found that the thermowell with helical strakes demonstrated no regular vortex shedding. While the flow behaviour varied significantly along the length of the thermowell it was observed that little or no time dependent changes occurred and the results were considered dynamically stable in all cuts along the length. The plots showing flow streamlines provided an excellent visualisation of the influence of the helical strakes. It's suggested that the strakes sufficiently disturb the flow in the wake region such that no regular vortices can form. The strakes also encouraged cross plane flow behaviour (along the thermowell length) to an extent that was not observed with the standard thermowell. It's thought that this process also helps to interfere with vortex formation.

During the study, the current design procedures and applications were briefly assessed. This highlighted that the application of the design codes can display potentially costly shortcomings if they are not fully understood for a specific environment and application. In light of this, the natural frequencies of both the standard and modified thermowells were calculated using a finite element method. This methodology showed a difference in excess of 20% from the theoretical value currently used to design thermowells.

The Power Code design rules provide large limitations upon a thermowell's safe application and this is mostly based upon issues with vortex induced vibrations. It can therefore be assumed that a thermowell presenting no vortex shedding is applicable to a larger range of applications.

The study completed took no account of the fluid - structure coupling. This is a phenomenon where the vibration of the structure changes the frequency and nature of the vortex shedding and both the fluid and structure behaviours influence each other. Many papers present this behaviour and show that resonance can result well outside a theoretical range. It is documented that resonance has been observed for frequency ratios between unity and two which, if considered, leads to a further restriction on thermowell operating ranges.

Due to the limitations of computing power and the level of mesh detail required, the modelling did not assess the full length of a thermowell and any tip effects. It assumed that the tip effects will be negligible given the long slender design and the study identified replicating flow behaviour which can be extrapolated along the thermowell's length.

7.1.1 Summarised Conclusions

- The standard thermowell design presented significant and regular vortex shedding. The predicted frequency was approximately 90Hz.
- The thermowell equipped with helical strakes displayed no regular vortex shedding. While behaviour varied along the length of the well, it was replicated and was considered to be dynamically stable.

- The natural frequency of thermowells is significantly under predicted by the current design rules.
- It has been observed that the addition of helical strakes greatly reduces vortex induction around the thermowell. For the specific modelled scenario there was no regular vortex behaviour. This correlates with other papers on the subject that all find that helical strakes reduce vortex shedding behaviour.
- The model showed a number of limitations. It did not consider the fluid - structure coupling and assumed that the thermowell was rigid. Only a reduced section of the wells were assessed due to the computing limitations and mesh density required.

8 References

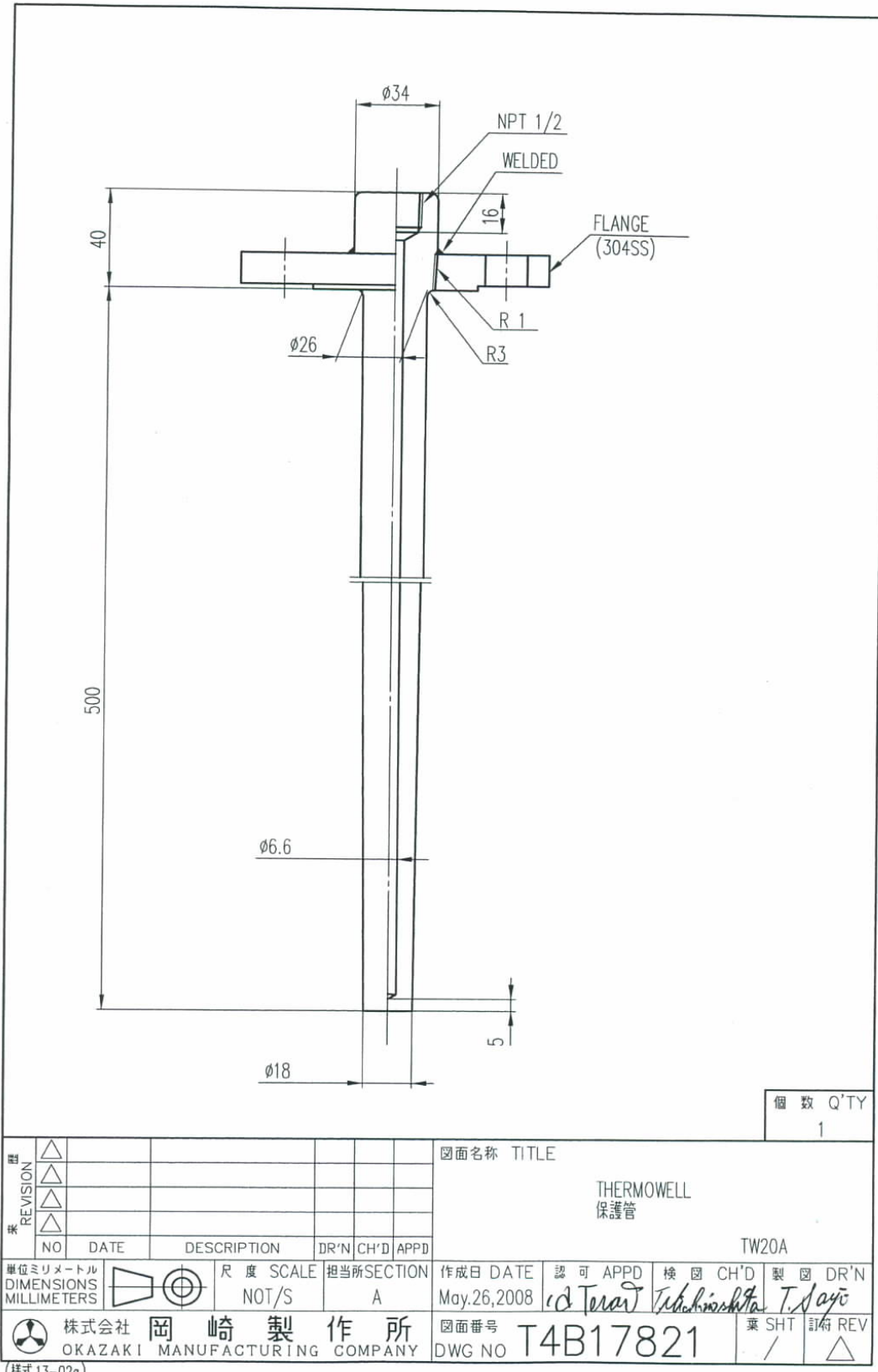
- [1] Murdock J.W., 'Power Test Code: Thermometer Wells', Journal of Engineering for Power (1959)

9 Liability/Indemnity

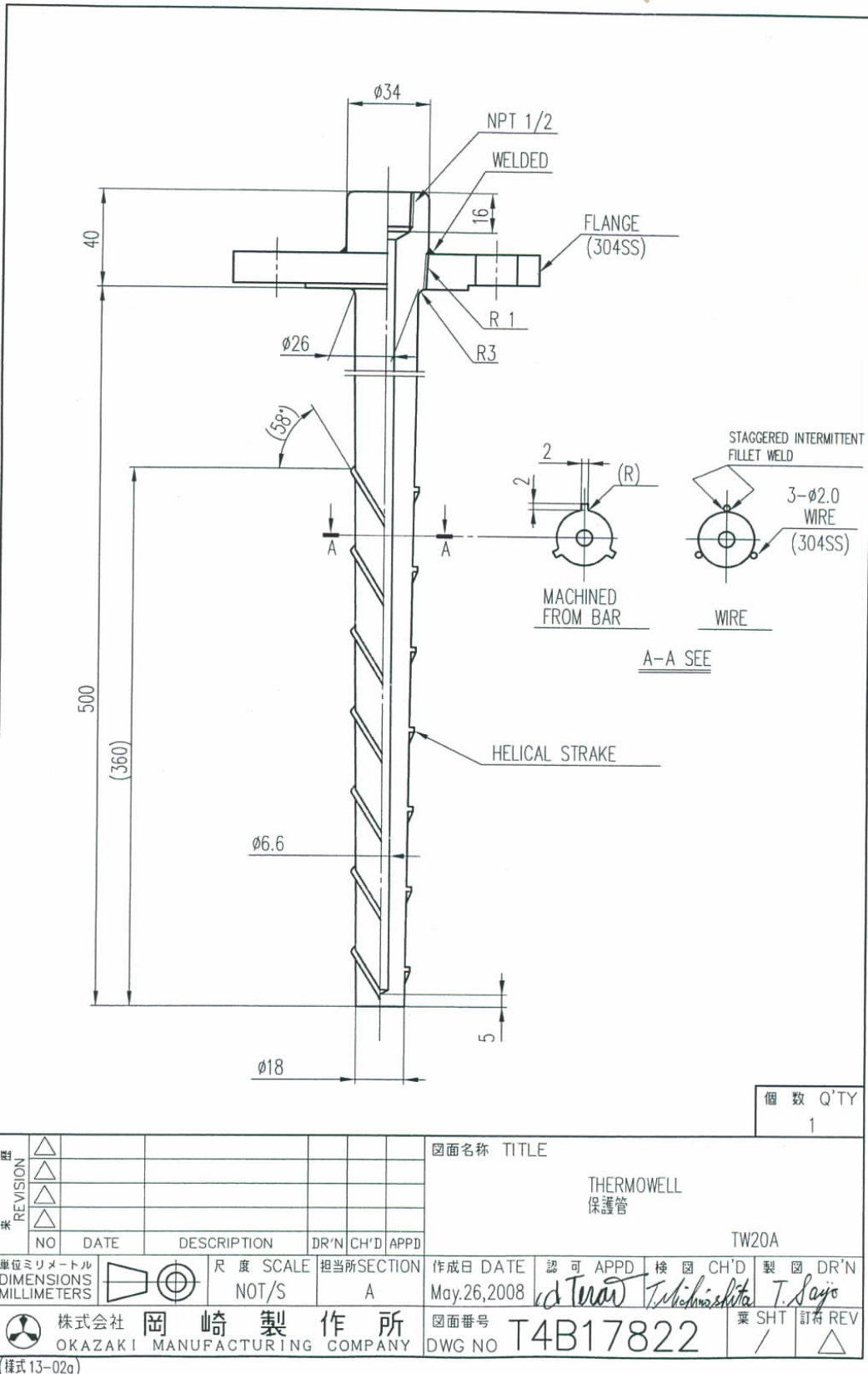
CDS undertakes to exercise all reasonable skill, care and diligence in the provision of the Work. CDS shall indemnify The Client in respect of loss or damage suffered by The Client to the extent that such loss or damage arises from the negligence or breach of statutory duty of CDS in carrying out the Work but not further or otherwise, provided that under no circumstances shall CDS be regarded as indemnifying The Client against any claims for loss of profit or loss of contracts that may be suffered by The Client. In any event CDS's total liability to The Client under this Clause shall be limited to the value of the total payment made to CDS under this Agreement. CDS shall not be liable for any loss or damage (other than death or personal injury caused by negligence on the part of CDS) arising from the action of any representative of The Client witnessing the tests and failing to comply with CDS's safety rules and regulations or the directions of the engineer in charge of the laboratory operations.

10 Appendix

10.1 Appendix – Drawing Number T4B17821



10.2 Appendix – Drawing Number T4B17822



2008-08050345

10.3 Appendix – Strouhal Frequency

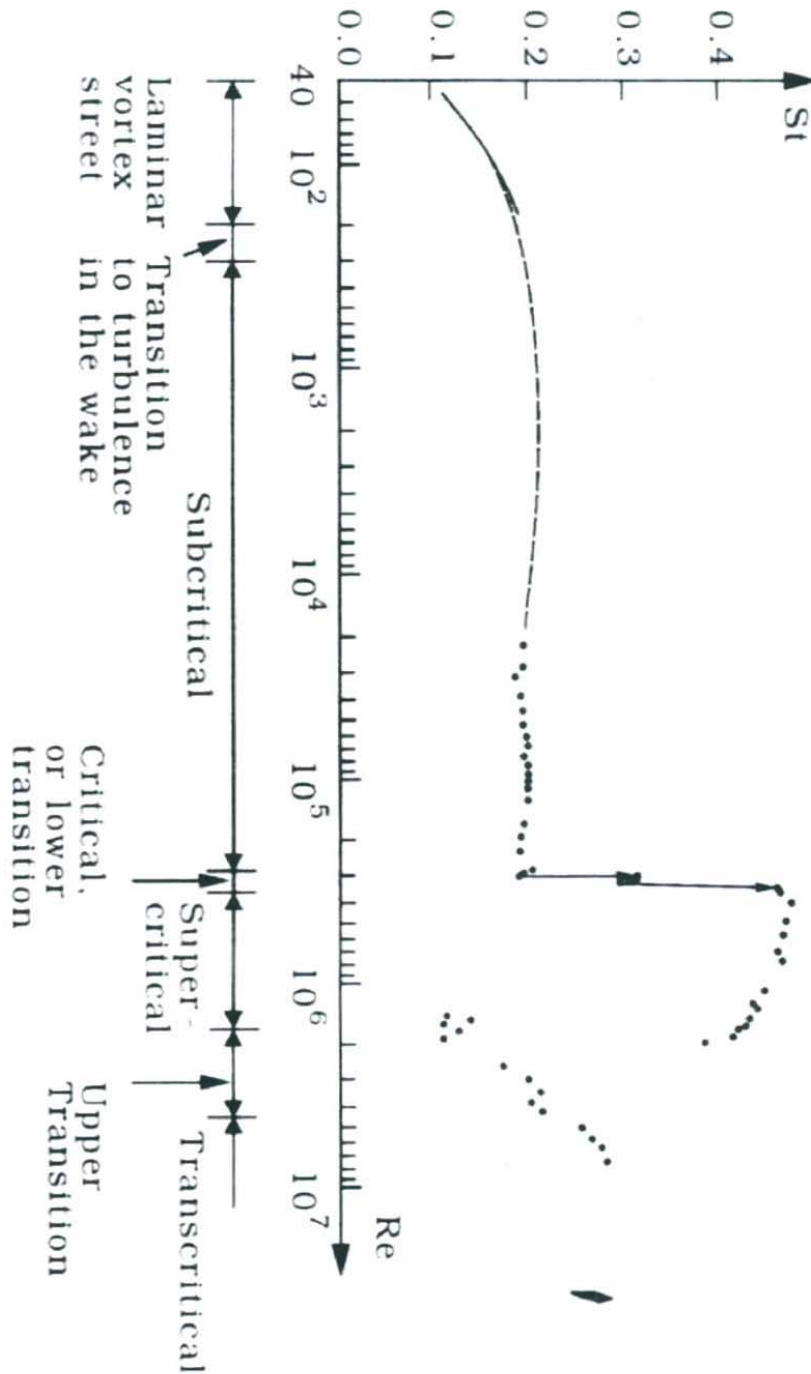
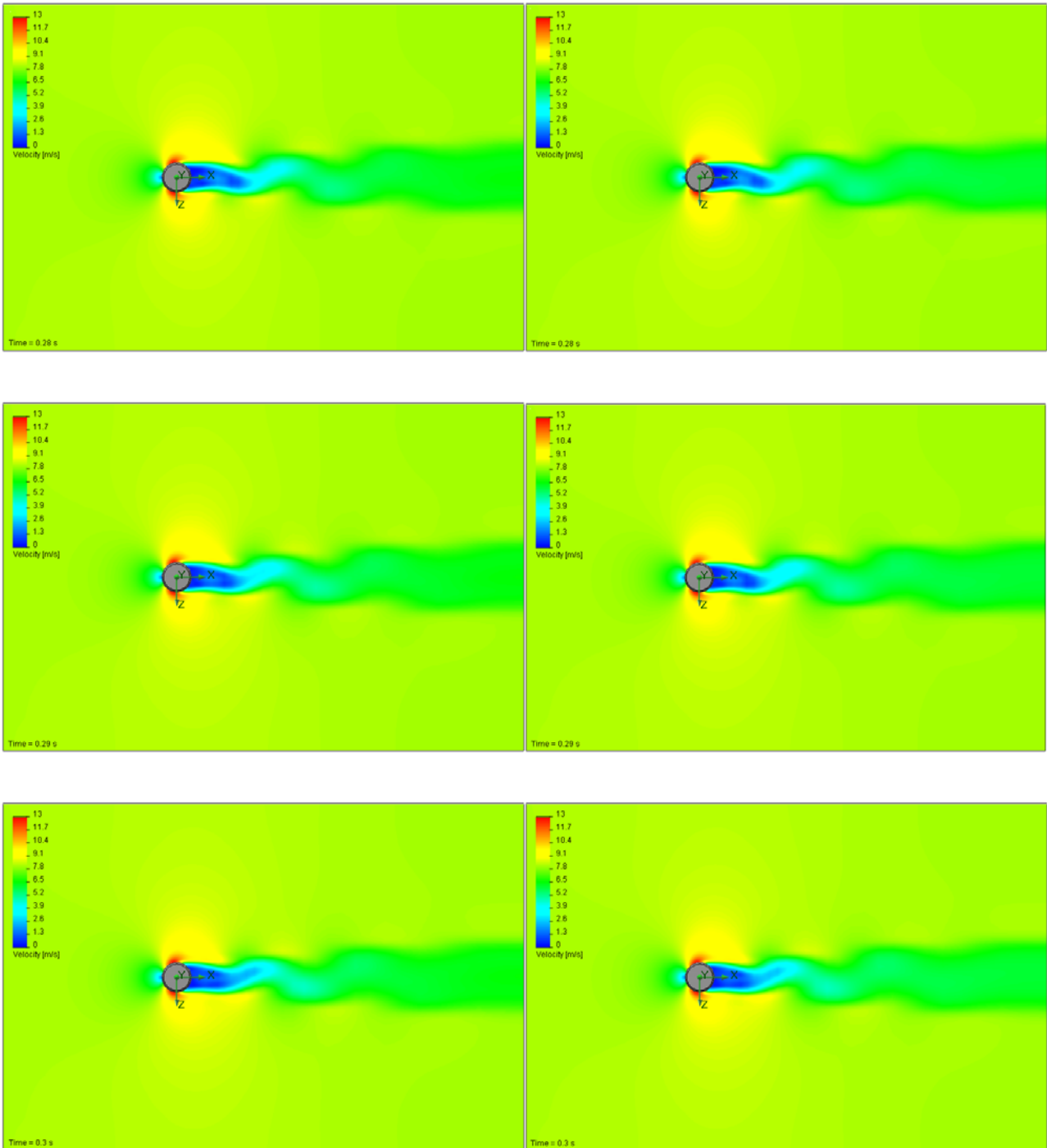


Figure 1.9 Strouhal number for a smooth circular cylinder. Experimental data from: Solid curve: Williamson (1989). Dashed curve: Roshko (1961). Dots: Schewe (1983).

Williamson, C.H.K. (1989): Oblique and parallel modes of vortex shedding in the wake of a circular cylinder at low Reynolds number. *J. Fluid Mech.*, 206:579-627

Roshko, A. (1961): Experiments on the flow past a circular cylinder at very high Reynolds number. *J. Fluid Mech.*, 10:345-356

10.4 Appendix – Smooth Thermowell Velocity Plots



10.5 Appendix – Straked Thermowell Velocity Plots

